

This document is confidential and is proprietary to the American Chemical Society and its authors. Do not copy or disclose without written permission. If you have received this item in error, notify the sender and delete all copies.

TiO₂ Nanotubes: Interdependence of Substrate Grain Orientation and Growth Rate

Journal:	<i>ACS Applied Materials & Interfaces</i>
Manuscript ID:	am-2014-07181p.R1
Manuscript Type:	Article
Date Submitted by the Author:	06-Dec-2014
Complete List of Authors:	Leonardi, Silvia; Technische Universität München, Physics Department E19 Russo, Valeria; Politecnico di Milano, Department of Energy and NEMAS - Center for NanoEngineered MAterials and Surfaces Li Bassi, Andrea; Politecnico di Milano, Department of Energy Di Fonzo, Fabio; Istituto Italiano di Tecnologia, Center for Nanoscience and Technology Murray, Thomas; SUNY Polytechnic Institute, Colleges of Nanoscale Science and Engineering Efstathiadis, Harry; SUNY Polytechnic Institute, Colleges of Nanoscale Science and Engineering Agnoli, Andrea; MINES ParisTech, Center for Materials Forming (CEMEF) Kunze-Liebhäuser, Julia; Leopold-Franzens-Universität Innsbruck, Institute of Physical Chemistry

SCHOLARONE™
Manuscripts

TiO₂ Nanotubes: Interdependence of Substrate Grain Orientation and Growth Rate

*Silvia Leonardi^a, Valeria Russo^b, Andrea Li Bassi^b, Fabio Di Fonzo^c, Thomas M. Murray^d, Harry Efstathiadis^d, Andrea Agnoli^e, and Julia Kunze-Liebhäuser^{*a,f}.*

(a) Department of Physics E19 and Institute for Advanced Study, Technische Universität München, James-Franck-Str. 1, 85748, Garching, Germany

(b) Department of Energy and NEMAS - Center for NanoEngineered MAterials and Surfaces, Politecnico di Milano, via Ponzio 34/3, 20133 Milan, Italy

(c) Center for Nano Science and Technology@PoliMi, Istituto Italiano di Tecnologia, via Pascoli 70/3, 20133 Milan, Italy

(d) Colleges of Nanoscale Science and Engineering, State University of New York Polytechnic Institute, 257 Fuller Road, Albany NY, 12203, USA

(e) MINES ParisTech, Center for Materials Forming (CEMEF), UMR CNRS 7635, BP 207, 06904 Sophia-Antipolis, France

(f) Institute of Physical Chemistry, University of Innsbruck, Innrain 52c, 6020 Innsbruck, Austria

1
2
3 ABSTRACT
4
5
6

7 Highly ordered arrays of TiO₂ nanotubes can be produced by self-organized anodic growth. It is
8 desirable to identify key parameters playing a role in the maximization of the surface area,
9 growth rate and nanotube lengths. In the present work, the role of the crystallographic orientation
10 of the underlying Ti substrate on the growth rate of anodic self-organized TiO₂ nanotubes in
11 viscous organic electrolytes in the presence of small amounts of fluorides is studied. A
12 systematic analysis of cross sections of the nanotubular oxide films on differently oriented
13 substrate grains was carried out by a combination of electron backscatter diffraction (EBSD) and
14 scanning electron microscopy (SEM). The characterization allows for a correlation between TiO₂
15 nanotube lengths and diameters and crystallographic parameters of the underlying Ti metal
16 substrate, such as planar surface densities. It is found that the growth rate of TiO₂ nanotubes
17 gradually increases with decreasing planar atomic density of the titanium substrate. Anodic TiO₂
18 nanotubes with the highest aspect-ratio form on Ti(-151) (which is close to Ti(010)), whereas
19 nanotube formation is completely inhibited on Ti(001). In the thin compact oxide on Ti(001), the
20 electron donor concentration and electronic conductivity are higher, which leads to a competition
21 between oxide growth and other electrochemical oxidation reactions, such as the oxygen
22 evolution reaction, upon anodic polarization. At grain boundaries between oxide films on
23 Ti(*hk*0), where nanotubes grow, and Ti(001), where thin compact oxide films are formed, the
24 length of nanotubes decreases most likely due to electron migration from TiO₂ on Ti(001) to
25 TiO₂ on Ti(*hk*0).
26
27
28
29
30
31
32
33
34
35
36
37
38
39
40
41
42
43
44
45
46
47
48
49
50
51

52
53 KEYWORDS
54

55 Anodic TiO₂ nanotubes, EBSD, self-organized anodic growth, growth rate, organic electrolyte
56
57
58
59
60

Introduction

Since the first report on anodic self-organized Al_2O_3 pore formation on Al substrates¹, anodic self-organized oxide nanostructures grown on valve metals have been intensely investigated. Anodic oxide films grown on valve metals have no or very low electronic conductivity, so that besides the ionic current responsible for oxide film growth, almost no electronic current, associated with side-reactions, such as the oxygen evolution reaction, taking place at the surface of the oxide film, can flow through the film. Self-organized anodic TiO_2 nanotube arrays²⁻⁴ are highly interesting materials among valve metal oxides, due to the combination of a regular and controllable nanoscale geometry with the various functional properties of titania, that make the material suitable for applications in e.g., electro-^{5,6} and photo-catalysis⁷, solar energy conversion^{8,9}, sensing¹⁰, biomedical devices^{11,12} and Li-ion batteries.¹³⁻¹⁵ A large variety of nanotube morphologies can be obtained by fine tuning the electrochemical anodization parameters. Effects of applied potential, anodization time, solution composition and pH on the resulting oxide properties have been reported.¹⁶ The proposed growth mechanisms for TiO_2 nanotube formation refer to a combination of flow and dissolution models.^{17,18} Self-organized anodic processes in highly-viscous electrolytes can lead to the formation of high aspect-ratio nanotubular TiO_2 arrays.¹⁶ In this regard, it is desirable to identify the key parameters playing a role in the maximization of the surface area, overall growth rate and nanotube lengths.

Nanotubular anodic TiO_2 growth in fluoride containing electrolytes has been extensively investigated since its discovery in 1999.² Compact anodic TiO_2 , formed in fluoride-free electrolytes, has also been thoroughly studied for a long time, a review is given in.²⁹ In the case

1
2
3 of compact anodic TiO₂ grown on Ti, it has been shown that the TiO₂ film thickness, donor
4 concentration and electronic conductivity depend on the crystallographic orientation of the Ti
5 substrate grains, and that the rate of ion transfer reactions (e.g., passive film growth) and electron
6 transfer reactions (e.g., oxygen evolution) differ from grain to grain.^{19–23} A combination of
7 electrochemical analysis with high spatial resolution and electron backscatter diffraction (EBSD)
8 has been employed to study the correlation between crystallographic orientation of the
9 underlying Ti metal substrate and the electrochemical behaviour of the compact anodic oxide
10 formed on top.²² Layer thickness and crystallinity of anodic compact TiO₂ were analyzed. It was
11 found that thin crystalline, electronically conductive oxide films are formed on Ti(001), whereas
12 thicker less crystalline films with lower electronic conductivity grow on Ti(*hk*0). A direct
13 consequence of the significant electron conductivity of the growing anodic TiO₂ films is that,
14 besides the ionic current responsible for film growth, an electronic current, associated with side-
15 reactions taking place at the surface of the oxide film, can flow through the film. Therefore, there
16 is a competition between oxide growth and other electrochemical oxidation side-reactions, being
17 mainly the oxygen evolution reaction.²⁹ For TiO₂ on Ti(001) anodic oxygen evolution takes
18 place at potentials >4 V, whereas on Ti(*hk*0) and misoriented grains oxide formation is the only
19 charge transfer reaction observed, which leads to the formation of thick passive films.²²

20
21
22
23
24
25
26
27
28
29
30
31
32
33
34
35
36
37
38
39
40
41
42
43
44 In an earlier paper the authors showed how the growth characteristics of anodic nanotubular
45 TiO₂ films, produced in an aqueous electrolyte solution of 1 M (NH₄)H₂PO₃ + 0.5 wt % NH₄F,
46 can be tailored by controlling the orientation of the underlying Ti metal substrate.²⁴ It was found
47 that open or partially capped amorphous TiO₂ nanotubes form on Ti(*hk*0) grains, where growth
48 of thick nanotubular oxide films was enabled. On Ti(001) grains, no open nanotubes but compact
49 oxide films were observed, exhibiting a mixed anatase and rutile nanocrystalline character with a
50
51
52
53
54
55
56
57
58
59
60

1
2
3 large degree of structural disorder.^{24,30} Except for this study,²⁴ only one paper describes retarded
4
5 nanotube growth on the Ti(001) surface.³¹ The results reported therein, even though interesting,
6
7
8 do not provide a detailed understanding of the interdependence of nanotube growth and grain
9
10 structure, resulting in deriving only qualitative conclusions.

11
12
13
14 In the present work, we report on the anodization of polycrystalline Ti metal surfaces in
15
16 glycerol-based electrolytes with small additions of fluorides and on the analysis of the growth
17
18 rates of anodic titania nanotubes on differently oriented Ti substrate grains. The organic
19
20 electrolyte with small amounts of fluorides was chosen to optimize the conversion efficiency by
21
22 slowing down the oxide dissolution rate and, at the same time, to fabricate nanotubes with a
23
24 more defined ripple-free geometry, as previously shown in studies on the nanotube growth
25
26 mechanism.¹⁸ The cross section analysis of TiO₂ nanotubes allowed the characterization of their
27
28 length as a function of the crystallographic orientation and the corresponding planar atomic
29
30 densities of the underlying Ti metal substrate, and provided information on the growth
31
32 mechanism.
33
34
35
36
37
38
39
40
41

42 **Experimental section**

43 **Reagent, solution and electrode materials**

44
45
46 TiO₂ nanotubes have been grown on polycrystalline Ti sheets of 1mm thickness (99.96%
47
48 purity, AdventMaterials Ltd., England) with an edge length of 1cm. Prior to the anodic
49
50 treatment, each Ti substrate was mechanically polished by using wet SiC grinding paper (grade
51
52 4000) followed by an electropolishing step in a mixture of methanol (purity ≥ 99.9%, Merck)
53
54
55
56
57
58
59
60

1
2
3 perchloric acid (HClO₄, 40%) (99.9% suprapure, Merck) and butoxyethanol (purity ≥ 99%, Alfa
4 Aesar).²⁵ For electropolishing, the Ti substrates were wrapped in teflon tape with an opening
5
6 providing an exposed area of ~80 mm² during the electropolishing treatment. A potential of 60 V
7
8 was applied for 5 minutes between the sample and a gold counter electrode. The electropolishing
9
10 solution was held between -20 and -40°C during the entire growth process. At the end of each
11
12 electropolishing treatment, all substrates were cleaned in ethanol (absolute grade emsure[®], VWR
13
14 Chemicals) in an ultrasonic bath (Sonorex, Bandelin Electronic) and rinsed with Milli-Q (DI
15
16 water (resistivity of 18.2 MΩ.cm at 25°C, Millipore). After two electropolishing cycles, the
17
18 teflon mask was removed and the samples were sonicated for 30 min in ethanol (99.9% empure,
19
20 VWR Chemicals) before rinsing with DI water. Prior to the anodization treatment, the Ti
21
22 substrates were further degreased by sonication in acetone, isopropanol and methanol,
23
24 thoroughly rinsed with DI water and finally dried in a nitrogen stream. Anodic growth of all
25
26 TiO₂ nanotube arrays presented in this paper was carried out in a mixed electrolyte solution of
27
28 glycerol (anhydrous, purity ≥ 99.95%, Merck) and 0.25wt % NH₄F (99.998 % purity, Merck).
29
30 All chemicals were used without further purification.
31
32
33
34
35
36
37
38
39

40 **Electrochemical synthesis and instrumentation**

41
42
43 A conventional two-electrode teflon electrochemical cell with a platinum gauze as counter
44
45 electrode was employed for the synthesis of the TiO₂ nanotubes. Prior to each experiment, the
46
47 cell was cleaned in Caro's acid (3:1 mixture of H₂SO₄ and H₂O₂) and thoroughly rinsed with DI
48
49 water. Nanotube growth was carried out at room temperature without stirring at a constant
50
51 voltage of 20 V for 6 hours by using a DC power supply (PS240 3D, Fluke). The final potential
52
53 was reached by ramping from 0 to 20 V with a ~1 V s⁻¹ rate. After anodic nanotube production,
54
55 each sample was thoroughly rinsed with DI water and dried in a nitrogen stream.
56
57
58
59
60

Surface analysis

Electron backscatter diffraction (EBSD): The inverse pole figure (IPF) of polycrystalline Ti and the related grain orientation map was obtained on a defined area of the metal substrates by EBSD. The IPF represents the stereographic projection leading to 32 crystallographic classes in six systems and shows the grain orientations characterizing the surface texture of the titanium substrate. The IPF shows how the selected direction in the sample reference frame is distributed in the reference frame of the crystal. The directions plotted are the stereographic projection of crystal directions parallel to the normal direction (ND), rolling direction (RD) or transverse direction (TD) in the sample. During the measurement, an amorphous native oxide of ~1.3-5.4 nm thickness was considered,²⁶ which is thin compared to the information depth of ~20 nm²² of EBSD and does therefore not lead to a decrease of pattern quality due to scattering. The area for the map was indicated by fiducial marks milled into the sample using a Ga beam with an accelerating voltage of 30 kV and a beam current of 21 nA. During milling, the surface was sealed with ink from a Sharpie pen to avoid contamination. After milling, the ink was removed by sonicating the sample in acetone followed by ethanol. The standard measurement configuration (45° pretilted specimen mount, Ted Pella Item 16355, 70° angle between electron beam and surface) with tilt correction was used to record a microstructural map of (50 x 50) μm² with a step size of 0.5 μm. A field-emission scanning electron microscope (FEI Nova NanoSEM600 Dualbeam, HKL Channel 5), with an acceleration voltage of 30 kV, a working distance of 12 – 15 mm, and a beam current of 0.64 nA, was used to collect the EBSD pattern. A set of three Euler angles φ_1 , Φ , and φ_2 is generally retrieved from EBSD analysis to fully determine the crystallographic orientation of grains in a three dimensional system. To describe the crystallographic texture in hcp systems, like Ti, either Miller-Bravais Indices $\{hkil\}$ or Miller

1
2
3 indices $\{hkl\}$ were used: The transformation from Euler space to the (hkl) planes was obtained
4
5 by applying a simple matrix multiplication.^{22,27} Planar surface densities were calculated for the
6
7 differently oriented Ti substrate surfaces using a modeling tool enclosed in the software
8
9 CrystalKit.
10

11
12
13 **Scanning Electron Microscopy (SEM):** All SEM analysis has been carried out with a Zeiss
14
15 Supra 40 field emission microscope. Cross section images of specific grains were acquired by
16
17 tilting the specimen mount to a 45° angle between the surface normal and the microscope
18
19 detector. The tilt was then corrected to determine the real nanotube lengths. For cross-section
20
21 SEM imaging, a home-made set up consisting of tungsten needles with tip dimensions of $10\ \mu\text{m}$
22
23 in diameter mounted on micro manipulators (Wentworth, model PVX-400) and equipped with an
24
25 optical microscope was used to scratch through grains on the anodized surface inside the area
26
27 previously mapped with EBSD.
28
29
30
31
32
33
34
35
36

37 **Results and discussion**

38

39
40 Figure 1 shows SEM micrographs of TiO_2 nanotubes grown on non-electropolished and on
41
42 electropolished Ti substrates. The TiO_2 nanotube array formed on the non-electropolished Ti
43
44 substrate is covered by a disordered capping layer (Figure 1a), which is typically observed for
45
46 organic electrolytes.²⁸ The crystallographic structure of the underlying metal substrate has no
47
48 influence on the nanotube growth rate. Based on statistical analysis of cross sections taken on
49
50 different areas, it is observed that the nanotubes have the same average length of $\sim 3\ \mu\text{m}$ all over
51
52 the surface (Figure 1c). Their length depends on the fluoride concentration and on the
53
54 anodization time, as reported earlier.¹⁶ The outer nanotube diameter and the side wall thickness,
55
56
57
58
59
60

1
2
3 both measured at the nanotube top, are ~ 50 nm and ~ 4 nm (see Figs. 1c and S1a in the
4
5 supporting information (SI)). The walls have a completely smooth morphology from top to
6
7 bottom (see Figure S1 in the SI). On electropolished substrates, a grain structure is clearly visible
8
9 and the capping layer that covers the topmost nanotube surface shows a different morphology on
10
11 different substrate grains (Figure 1b). At least four zones with different growth rates are
12
13 identified (see Figure S2 in the SI) in which nanotube lengths range from ~ 1.5 μm to ~ 3.1 μm
14
15 (see Figure 1d,e). The nanotube outer diameters range from ~ 30 to ~ 90 nm, where the longest
16
17 nanotubes (3.1 μm) have the smallest diameter of ~ 30 nm and the shorter nanotubes (1.5 and
18
19 1.7 μm) have diameters of ~ 90 and 75 nm, respectively. The morphology of the tube walls is
20
21 mainly smooth, but on some grains ripples are observed at the nanotube bottoms that form at
22
23 later growth stages (Figure 1d).
24
25
26
27
28
29
30
31
32
33
34
35
36
37
38
39
40
41
42
43
44
45
46
47
48
49
50
51
52
53
54
55
56
57
58
59
60

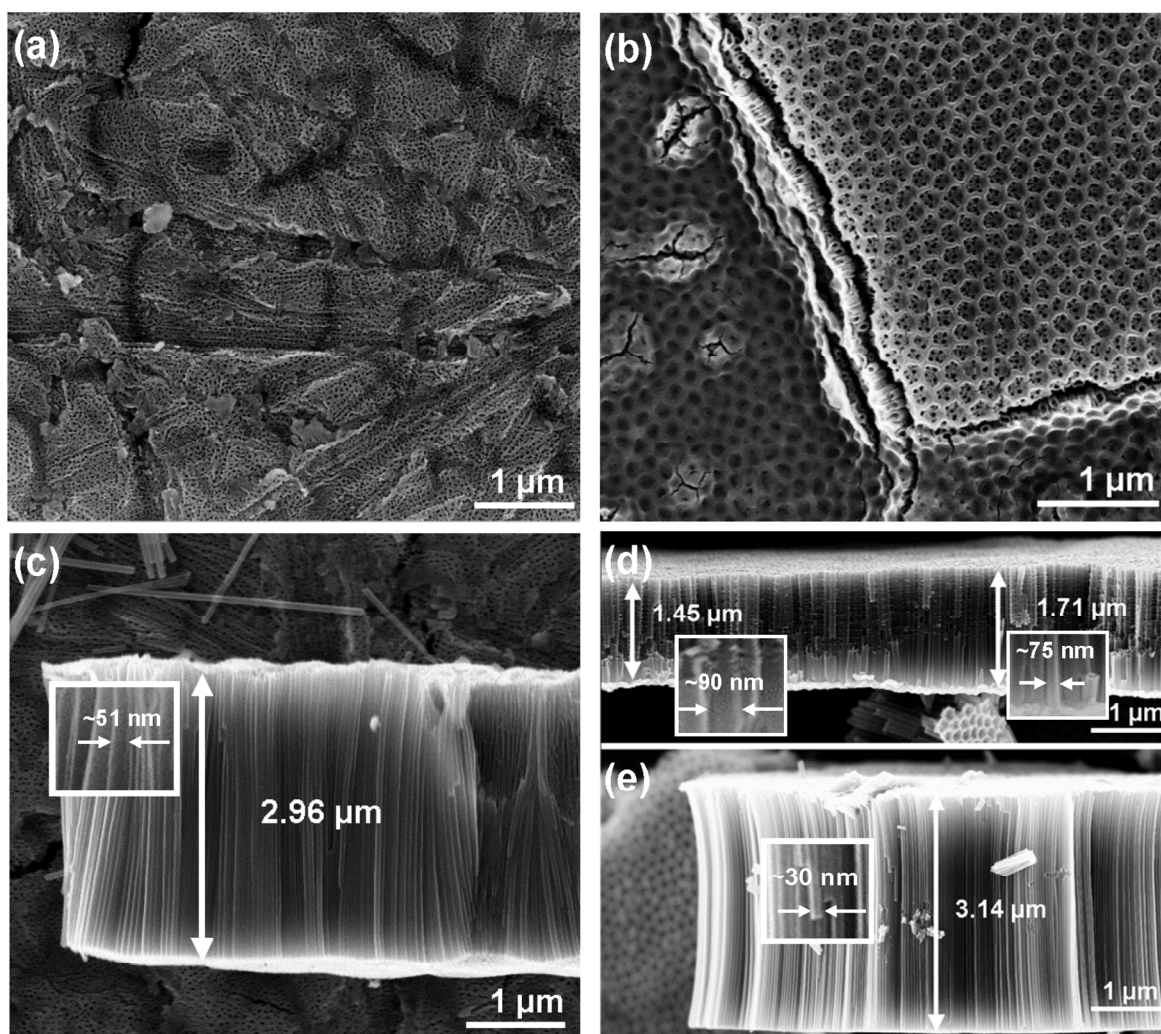


Figure 1: SEM top views and cross-sections of TiO₂ nanotubes grown in glycerol with 0.25wt.% NH₄F at 20 V for 6 hours on non-electropolished (a,c) and on electropolished (b,d,e) Ti substrates. In panel (d), the nanotube layer is flipped upside down, the nanotube bottoms show ripples (see left inset in (d)).

In order to gain a better understanding of the factors that lead to the formation of high-aspect ratio TiO₂ nanotubes in organic electrolytes and, in particular, of the role the substrate grain orientations play, the Ti metal substrate was characterized by EBSD after electropolishing and prior to anodization. The inverse pole figure (IPF) of the Ti metal substrate, detected with EBSD, is depicted in Figure 2. Crystallographic orientations of the planes characterizing the Ti substrate texture are given by the color legend of the corresponding orientation distribution map (Figure

2). To evaluate the growth rate dependence of TiO_2 nanotubes on the orientation of the underlying substrate (see Figure 1), cross sections of TiO_2 nanotubes grown on differently oriented substrate grains were taken to correlate nanotube length and substrate orientation. The positions where cross-sections were analyzed are indicated on the EBSD map in Figure 2.

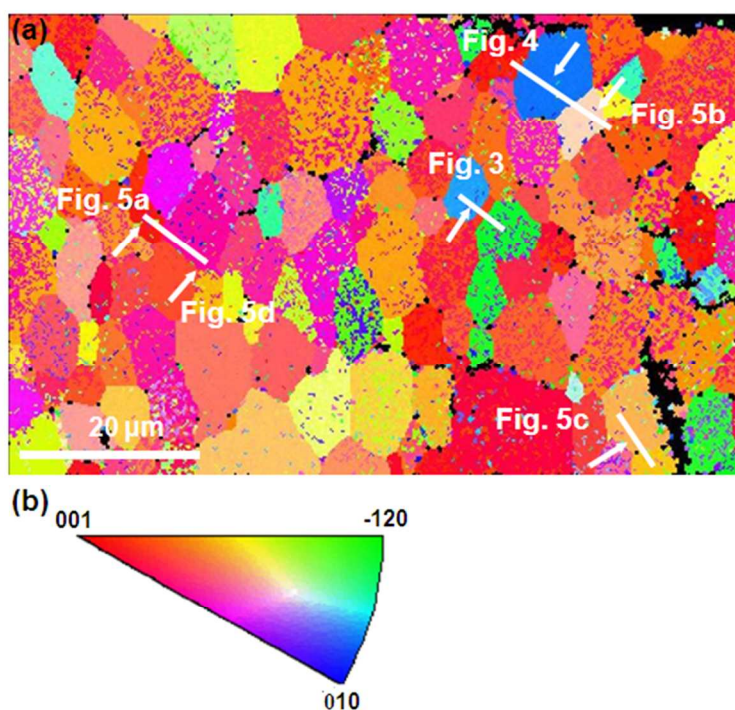


Figure 2: (a) Inverse pole figure (IPF) map of the area where cross sections of the nanotubular film are investigated with SEM, cross sections are marked by white lines. (b) color legend for the IPF explaining the crystallographic orientations (orientations of the vertices refer to substrate planes).

Figure 3 shows a SEM cross-section through TiO_2 nanotubes formed on substrate grains identified as $\text{Ti}(-160)$, $\text{Ti}(001)$, and $\text{Ti}(-120)$ planes. These orientations correspond to the light blue, red, and green areas of the map (Fig 3b). Anodization of titanium metal grains with $\text{Ti}(-160)$ and $\text{Ti}(-120)$ orientations leads to the formation of ~ 650 and ~ 610 nm long TiO_2

nanotubes, whereas on the low index plane Ti(001) (red area in the color legend) an 80 nm thick compact oxide film with no trace of porosity, chemical etching or self-organized nanotube formation is grown. A pronounced grain boundary effect can be noticed where nanotube lengths on Ti(-160) and Ti(-120) oriented grains dramatically decrease close to the compact oxide layer formed on Ti(001).

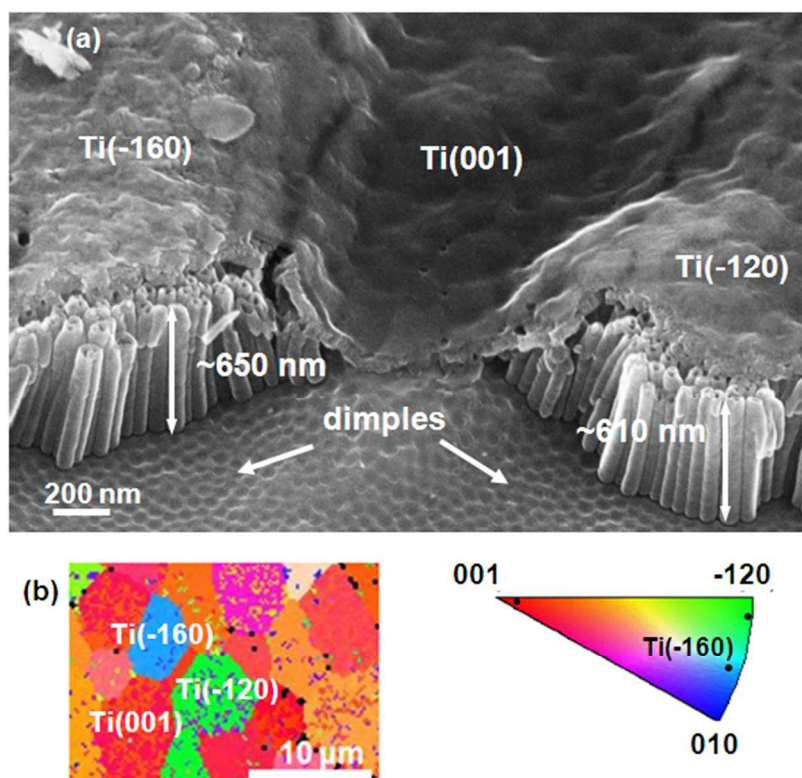


Figure 3: (a) Cross section of anodic TiO₂ nanotubes grown in glycerol with 0.25 wt.% NH₄F at 20 V for 6 hours on Ti(-160), Ti(001) and Ti(-120) oriented grains. (b) EBSD map and stereographic triangle showing the positions of substrate grains underlying the nanotubular oxides.

Figure 4 depicts a SEM cross section of nanotubular anodic oxide formed on a Ti(-151) oriented grain, located in the blue area of the orientation distribution map, where the TiO₂ nanotube

1
2
3 length reaches a value of ~ 920 nm. This indicates that the nanotube growth rate is enhanced on
4
5 substrate orientations such as Ti(-151), when compared to Ti(001). It is important to note that, in
6
7 the present study, the nanotube lengths measured on the surface that was mapped with EBSD
8
9 prior to nanotube growth were smaller compared to the lengths of nanotubes grown on Ti metal
10
11 substrates right after electropolishing under the same growth conditions. This effect is most
12
13 likely due to the treatment of the surface during milling with the Ga beam.
14
15
16
17
18
19
20
21
22
23
24
25
26
27
28
29
30
31
32
33
34
35
36
37
38
39
40
41
42
43
44
45
46
47
48
49
50
51
52
53
54
55
56
57
58
59
60

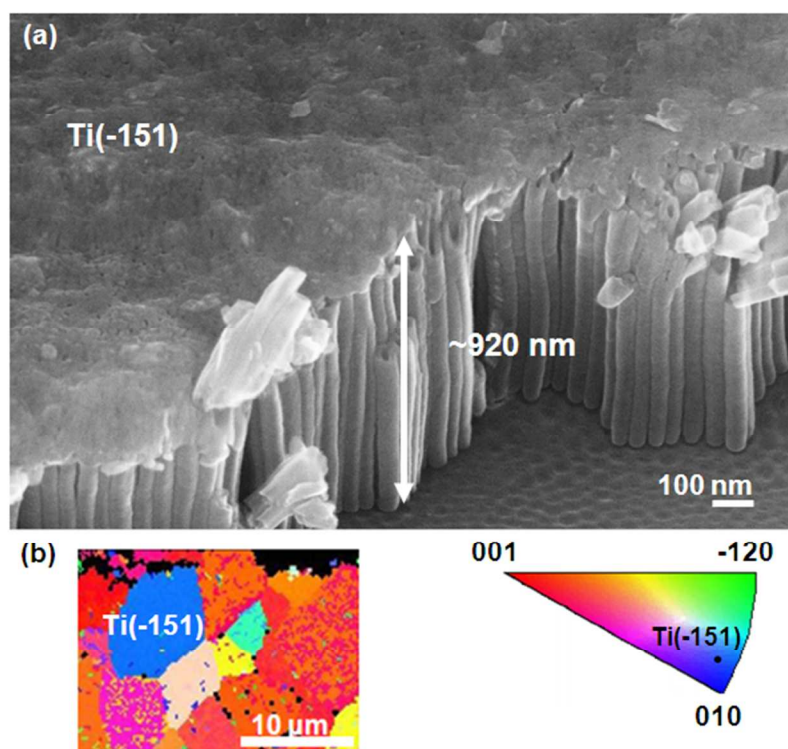


Figure 4: (a) SEM cross section of anodic TiO_2 nanotubes grown in glycerol with 0.25 wt.% NH_4F at 20 V for 6 hours on a Ti(-151) oriented grain. (b) EBSD map and stereographic triangle showing the position of the substrate grain underlying the nanotubular oxide.

Analysis of the thickness of the titania nanotube films on different substrate grain orientations in the mapped area allows correlation of the substrate grain orientation with the growth rate. Figure 5 depicts SEM micrographs of six different grains from the IPF and the corresponding positions in the stereographic triangle. Clearly, different nanotube lengths are measured for the different substrate grain orientations. It is observed that short nanotubes of only 175 nm length covered with a thick compact capping layer are grown on approximately Ti(001) oriented substrate grains, such as on Ti(017) (Figure 5a). On Ti(134) and Ti(115) oriented grains, nanotube lengths reach values of 290 and ~330 nm, respectively (Figure 5b).

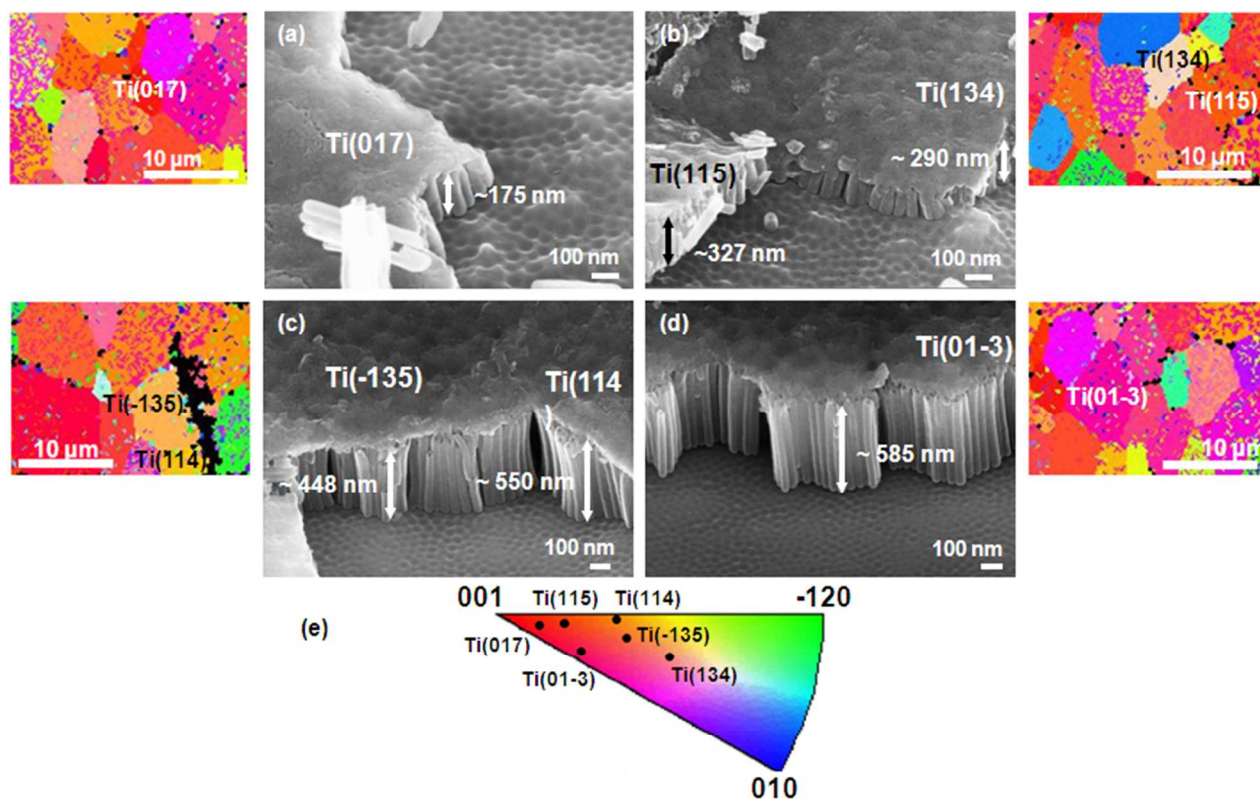


Figure 5: SEM cross sections of TiO₂ nanotubes grown in glycerol with 0.25 wt % NH₄F at 20V for 6 hours on differently oriented grains: (a) Ti(017), (b) Ti(115) and Ti(134), (c) Ti(-135) and Ti(114) and (d) Ti(01-3) with the corresponding IPF maps. (e) Stereographic triangle showing the positions of substrate grains underlying the nanotubular oxides.

On Ti(-135) and Ti(114) the growth rate is increased, and nanotube lengths of ~450 and 550 nm are obtained (Figure 5c). A further increase of the growth rate is observed for nanotubes grown on Ti(01-3) oriented grains, where 585 nm thick nanotubular films are formed (Figure 5d). As the thickness of the nanotube films increases, the thickness of the topmost capping layer decreases from ~60 nm on Ti(017) to less than ~20 nm on Ti(01-3).

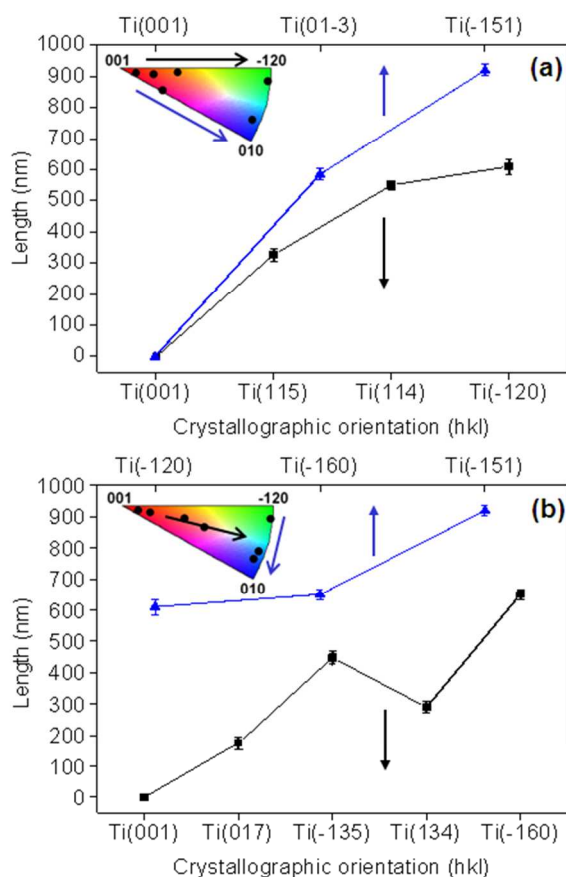


Figure 6: TiO₂ nanotube lengths for anodic films grown in glycerol with 0.25wt% NH₄F for 6 hours at 20V on differently oriented substrate grains (standard deviations refer to length variations inside the same substrate grain). Change of plane orientations (a) along upper (black curve) and lower (blue curve) edges of the stereographic triangle, and (b) from (-120) to (010) (blue curve) and through the high-index inner planes (black curve) of the stereographic triangle.

1
2
3 In Figure 6, all nanotube lengths measured on differently oriented substrate grains are
4 summarized. Figure 6 shows that nanotube growth rates are smallest on approximately (001)
5 oriented Ti substrate grains. Growth rate increases when the substrate grain orientation is
6 changed by moving along the upper and lower edges of the stereographic triangle, (with higher
7 growth rates observed for the lower edge, black and blue curve in Figure 6a). Growth rates are
8 considerably higher on grains with orientations belonging to the triangle edge connecting the
9 Ti(-120) and Ti(010) vertices, where nanotube lengths are never shorter than ~600 nm (blue line
10 in Figure 6b). When substrate grain orientations change following a virtual line through the
11 center of the stereographic triangle (black line in Figure 6b), the trend is not continuous because
12 a lower growth rate is observed for TiO₂ nanotubes grown on Ti(134).
13
14
15
16
17
18
19
20
21
22
23
24
25
26
27

28 The correlation of Ti substrate grain orientation and its corresponding atomic planar density
29 calculated as number of atoms per surface area with TiO₂ nanotube lengths, shows higher
30 nanotube growth rates for lower planar atomic densities (Figure 7). It is known that TiO₂
31 nanotube growth starts with the formation of a compact oxide layer which is first chemically
32 etched by the fluorides in the electrolyte, leading to the formation of an unordered porous oxide
33 layer. After this initial phase, a self-organized growth of TiO₂ nanotubes takes place.²⁸
34 Consequently, the nature of the compact oxide film formed prior to nanotube formation plays an
35 important role for self-organized nanotube growth. As mentioned in the introduction, compact
36 anodic oxide grown on Ti(001) is characterized by the highest electronic conductivity which
37 leads to an enhanced oxygen evolution at the expense of oxide layer formation.^{22,29} Our findings
38 demonstrate that no TiO₂ nanotube growth takes place on Ti(001) substrate surfaces, which
39 confirms our previous studies.²⁴
40
41
42
43
44
45
46
47
48
49
50
51
52
53
54
55
56
57
58
59
60

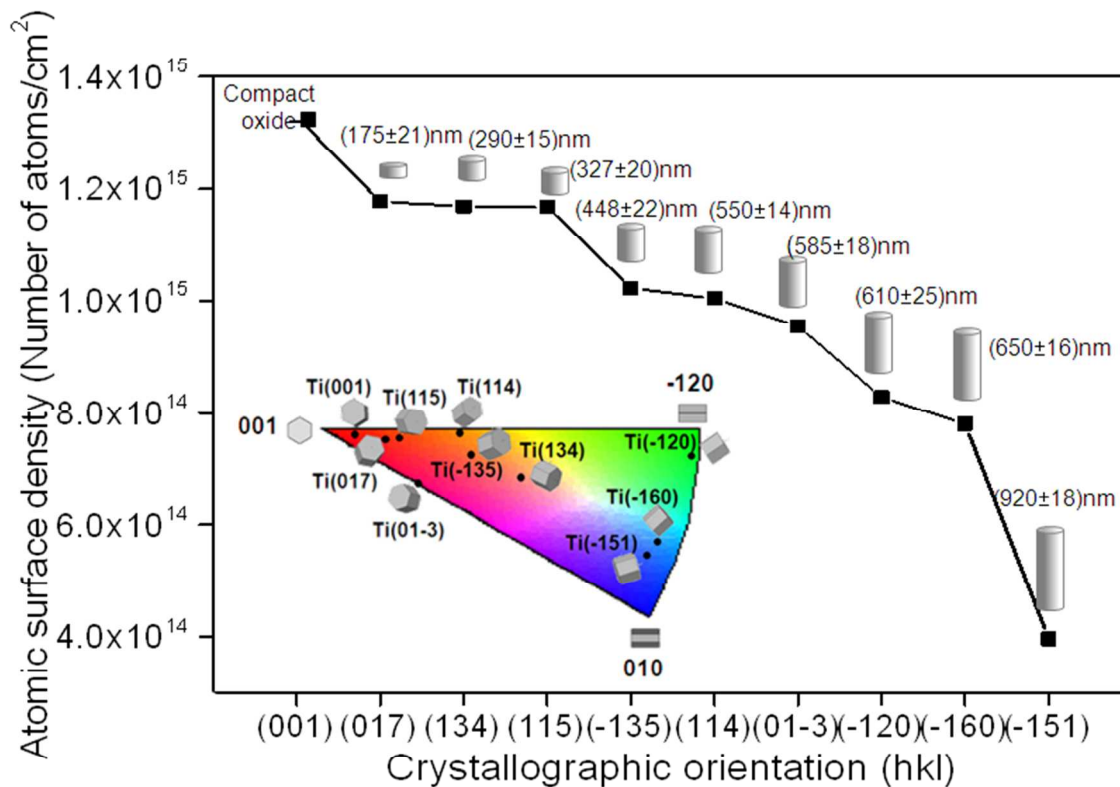


Figure 7: Atomic surface densities of Ti metal substrate planes and their correlation with TiO₂ nanotube lengths (standard deviations refer to length variations inside the same grain), connecting lines are inserted as guide for the eye. Inset: orientation of hexagonal 3D unit cells of Ti substrate grains determined from Euler angles obtained with EBSD.

It is important to note that a total absence of nanotubular features in the anodic film is only observed on a small portion of the Ti(001) grain narrowed between nanotube films on Ti(-160) and Ti(-120), whereas on a wider region of the same grain, dimples have formed. These dimples originate from TiO₂ nanotubes formed at the metal/oxide interface during the anodic self-organization process that were mechanically removed from the surface upon preparation of the cross-section (see arrows in Figure 3). A possible explanation for this finding could be the limited lateral resolution of the EBSD map; the system is very sensitive to small changes in the

1
2
3 crystallographic orientation, which might lead to nanotube growth on approximately (001)
4 oriented substrate grains (see e.g., Figure 5a).
5
6
7

8
9 The pronounced grain boundary effect, where nanotube lengths on Ti(-160) and Ti(-120)
10 oriented grains decrease at the boundary with the compact oxide layer formed on Ti(001), can be
11 explained by a change of electronic properties of TiO₂ grown on differently oriented substrate
12 grains: Davepon et al.²³ provided evidence that the electron concentration in the oxide film
13 formed on a given grain is not homogeneous, but exhibits gradients across grain boundaries, if
14 the film grown on an adjacent grain has a significantly different conductivity. According to these
15 authors, this observation is proof for lateral electron migration across the oxide. For the case of
16 decreasing TiO₂ nanotube length at grain boundaries with compact TiO₂ on Ti(001), lateral
17 electron migration can occur from TiO₂ grown on Ti(001) to TiO₂ grown on Ti(*hk*0) leading to
18 an increased electronic conductivity of TiO₂, and thus to a decrease of oxide growth rate, at the
19 grain boundary.
20
21
22
23
24
25
26
27
28
29
30
31
32
33
34
35
36
37
38

39 **Conclusions**

40
41
42
43 Electron backscatter diffraction and scanning electron microscopy were used to investigate the
44 growth rate of anodic, self-organized nanotubular titania in organic electrolytes and its
45 dependence on the crystallographic orientations of the underlying Ti substrate grains. It was
46 found that TiO₂ nanotubes with the highest-aspect ratio are formed on Ti(-151), whereas
47 compact TiO₂ films grow on Ti(001). It was observed that the growth rate of TiO₂ nanotubes
48 gradually increases with decreasing planar atomic density of the titanium substrate. TiO₂
49 nanotube length decreases at grain boundaries between compact oxide films formed on Ti(001)
50
51
52
53
54
55
56
57
58
59
60

1
2
3 and nanotube forming films on Ti(*hk0*) due to lateral electron migration from TiO₂ with higher
4
5 electron concentration present on Ti(001) to TiO₂ with lower electron concentration present on
6
7 Ti(*hk0*).
8
9

10 11 12 13 14 ASSOCIATED CONTENT

15
16
17
18 **Supporting Information:** Figure S1: Details of TiO₂ nanotube morphology. Figure S2: On
19
20 electropolished substrates, the capping layer that covers the topmost nanotube surface shows a
21
22 different morphology on differently oriented substrate grains. This material is available free of
23
24 charge via the Internet at <http://pubs.acs.org>.
25
26
27
28
29
30

31 AUTHOR INFORMATION

32 33 34 **Corresponding Author**

35
36 * Julia Kunze-Liebhäuser, julia.kunze@uibk.ac.at
37

38 39 **Author Contributions**

40
41 The manuscript was written through contributions of all authors. All authors have given approval
42
43 to the final version of the manuscript.
44
45
46
47
48
49

50 51 **Funding Sources**

52
53 The authors thank the DFG (project KU 2397/1-1), and the Technische Universität München
54
55 (TUM) Institute for Advanced Study, funded by the German Excellence Initiative for financial
56
57 support.
58
59
60

1
2
3
4
5
6
7
8
9
10
11
12
13
14
15
16
17
18
19
20
21
22
23
24
25
26
27
28
29
30
31
32
33
34
35
36
37
38
39
40
41
42
43
44
45
46
47
48
49
50
51
52
53
54
55
56
57
58
59
60

ACKNOWLEDGMENT

We thank Dr. Alessandro Luzio of the Italian Institute of Technology for providing the set-up and expertise in cross-section preparation.

REFERENCES

- (1) Masuda, H.; Fukuda, K. Ordered Metal Nanohole Arrays Made by a Two-Step Replication of Honeycomb Structures of Anodic Alumina. *Science* **1995**, 268, 1466-1468.
- (2) Zwilling, V.; Darque-Ceretti, E.; Boutry-Forveille, A.; David, D.; Perrin, M.Y.; Aucouturier M. Structure and Physicochemistry of Anodic Oxide Films on Titanium and TA6V Alloy. *Surf. Interface Anal.* **1999**, 27, 629-637.
- (3) Zwilling, V.; Aucouturier, M.; Darque-Ceretti, E. Anodic Oxidation of Titanium and TA6V Alloy in Chromic Media. An Electrochemical Approach. *Electrochim. Acta* **1999**, 45, 921-929.
- (4) Beranek, R.; Hildebrand, H.; Schmuki, P. Self-Organized Porous Titanium Oxide Prepared in H₂SO₄/HF Electrolytes. *Electrochem. Solid-State Lett.* **2003**, 6, B12-B14.
- (5) Macak, J. M.; Tsuchiya, H.; Bauer, S.; Schmuki, P.; Barczuk, P.; Nowakoska, M.Z.; Chojak, M.; Kulesza, P.J. Self-organized Nanotubular TiO₂ Matrix as Support for Dispersed Pt/Ru Nanoparticles, Enhancement of the Electrocatalytic Oxidation of Methanol. *Electrochem. Commun.* **2005**, 7, 1417-1422.
- (6) Hahn, R.; Ghicov, A.; Tsuchiya, H.; Macak, J. M.; Muñoz, A. G. and Schmuki, P. Lithium-Ion Insertion in Anodic TiO₂ Nanotubes Resulting in High Electrochromic Contrast. *Physica Status Solidi A* **2007**, 204, 1281-1285.

- 1
2
3
4
5
6
7
8
9
10
11
12
13
14
15
16
17
18
19
20
21
22
23
24
25
26
27
28
29
30
31
32
33
34
35
36
37
38
39
40
41
42
43
44
45
46
47
48
49
50
51
52
53
54
55
56
57
58
59
60
- (7) Kontos, A. G., A; Kontos, I.; Tsoukleris, D. S.; Likodimos, V.; Kunze, J.; Schmuki, P.; Falaras P. Photo-Induced Effects on Self-organized TiO₂ Nanotube Arrays: the Influence of Surface Morphology. *Nanotechnology* **2009**, 20, 045603.
- (8) Ghicov, A.; Albu, S. P.; Hahn, R.; Kim, D.; Stergiopoulos, T.; Kunze, J.; Schiller, C.-A.; Falaras, P.; Schmuki, P. TiO₂ Nanotubes in Dye-Sensitized Solar Cells: Critical Factors for the Conversion Efficiency. *Chem. Asian J.* **2009**, 4, 520-525.
- (9) Macak, J. M.; Tsuchiya ; Ghicov, A.; Schmuki, P. Dye-sensitized Anodic TiO₂ Nanotubes. *Electrochem. Commun* **2005**, 7, 1133-1137.
- (10) Varghese, O. K.; Gong, D.; Paulose ; Ong, K. G.; Grimes, C. A. Hydrogen Sensing Using Titania Nanotubes. *Sensors and Actuators B* **2003**, 93, 338-344.
- (11) Tsuchiya, H.; Macak, J. M.; Müller, L.; Kunze, J.; Müller, F.; Greil, P.; Virtanen, S.; Schmuki, P. Hydroxyapatite Growth on Anodic TiO₂ Nanotubes. *J. Biomed. Mater. Res.* **2006**, 77A, 534-541.
- (12) Kunze, J.; Müller, L.; Macak, J. M.; Greil, P.; Schmuki, P.; Müller, F. A. Time-dependent Growth of Biomimetic Apatite on Anodic TiO₂ Nanotubes. *Electrochim. Acta* **2008**, 53, 6995-7003.
- (13) Brumbarov, J.; Kunze-Liebhäuser, J. Silicon on Conductive Self-organized TiO₂ Nanotubes – A High Capacity Anode Material for Li-ion batteries. *J. Power Sources* **2014**, 558, 129-133.

- 1
2
3 (14) Wu, Q.L.; Li, J.; Deshpande, R.D.; Subramanian, N.; Rankin, S.E.; Yang, F.; Cheng, Y.-T.
4
5 Aligned TiO₂ Nanotube Arrays as Durable Lithium-Ion Battery Negative Electrodes. *J.*
6
7
8 *Phys. Chem. C* **2012**, 116, 18669-18677.
9
10
11 (15) Fang, H.-T.; Liu, M.; Wang, D.-W.; Sun, T.; Guan, D.-S.; Li, F.; Zhou, J.; Sham, T.-K.;
12
13 Cheng, H.-M. Comparison of the Rate Capability of Nanostructured Amorphous and
14
15 Anatase TiO₂ for Lithium Insertion Using Anodic TiO₂ Nanotube Arrays. *Nanotechnology*
16
17
18 **2009**, 20, 225701.
19
20
21 (16) Roy, P.; Berger, S.; Schmuki, P. TiO₂ Nanotubes: Synthesis and Applications. *Angew.*
22
23
24 *Chem. Int. Ed.* **2011**, 50, 2904-2939.
25
26
27 (17) Le Clere, D.J.; Valota, A.; Skeldon, P.; Thompson, G.E.; Berger, S.; Kunze, J.; Schmuki, P.;
28
29 Habazaki, H.; Nagata, S. Tracer Investigation Of Pore Formation In Anodic Titania. *J.*
30
31
32 *Electrochem. Soc.* **2008**, 155, C487-C494.
33
34
35 (18) Berger, S.; Macak, J.M.; Kunze, J.; Schmuki, P. High-efficiency Conversion of Sputtered Ti
36
37
38 Thin Films into TiO₂ Nanotubular Layers. *Electrochem. Solid-State Lett.* **2008**, 11, C37-
39
40
41 C40.
42
43
44 (19) Schultze, J.W.; Kudelka, S. Microtechniques Open Doorways to a New Understanding of
45
46
47 Electrochemical Systems. *Interface* **1997**, 6, 28.
48
49
50 (20) Kudelka, S.; Schultze, J.W. Photoelectrochemical Imaging and Microscopic Reactivity of
51
52
53 Oxidised Ti. *Electrochim. Acta* **1997**, 42, 2817-2825.
54
55
56
57
58
59
60

- 1
2
3
4
5
6
7
8
9
10
11
12
13
14
15
16
17
18
19
20
21
22
23
24
25
26
27
28
29
30
31
32
33
34
35
36
37
38
39
40
41
42
43
44
45
46
47
48
49
50
51
52
53
54
55
56
57
58
59
60
- (21) Kudelka, S.; Michaelis, A.; Schultze, J.W. Effect of Texture and Formation Rate on Ionic and Electronic Properties of Passive Layers on Ti Single Crystals. *Electrochim. Acta* **1996**, 41, 863-870.
- (22) König, U.; Davepon, B. Microstructure of Polycrystalline Ti and its Microelectrochemical Properties by Means of Electron-Backscattering Diffraction (EBSD). *Electrochim. Acta* **2001**, 47, 149-160.
- (23) Davepon, B.; Schultze, J.W.; König, U.; Rosenkranz, C. Crystallographic Orientation of Single Grains of Polycrystalline Titanium and Their Influence on Electrochemical Processes. *Surf. Coat. Technol.* **2003**, 169-170, 85-90.
- (24) Leonardi, S.; Li Bassi, A.; Russo, V.; Di Fonzo, F.; Paschos, O.; Murray, T.M.; Efstathiadis, H.; Kunze, J. TiO₂ Nanotubes: Interdependence of Substrate Grain Orientation and Growth Characteristics, *J. Phys. Chem. C* **2012**, 116, 384-392.
- (25) Arsov, L. D. Dissolution Electrochimique des Films Anodiques du Titane dans l'Acide Sulfurique. *Electrochim Acta* **1985**, 30, 1645-1657.
- (26) Schultze, J.W.; Lohrengel, M.M. Stability, Reactivity and Breakdown of Passive Films. Problems of Recent and Future Research. *Electrochimica Acta* **2000**, 45, 2499-2513.
- (27) Kallend, J.S.; Kocks, U.F.; Rollett, A.D.; Wenk, H.-R.; Operational Texture Analysis. *Mater. Sci. Eng. A* **1991**, 132, 1-11.
- (28) Berger, S.; Kunze, J.; Schmuki, P.; LeClere, D.; Valota, A.; Skeldon, P.; Thompson, G. A Lithographic Approach to Determine Volume Expansion Factors During Anodization: Using

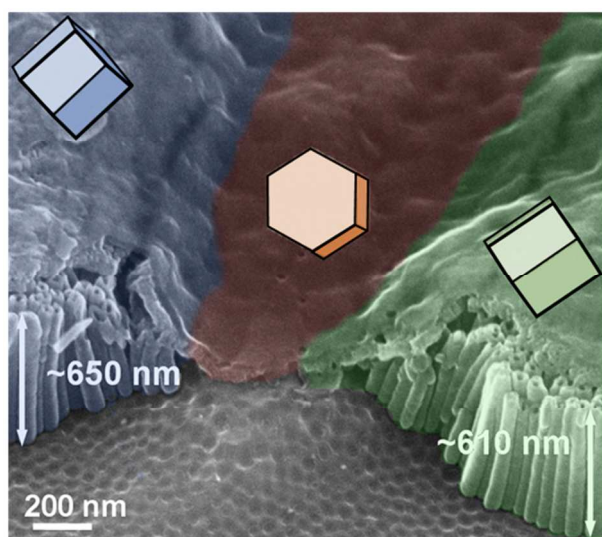
1
2
3 the Example of Initiation and Growth of TiO₂-Nanotubes. *Electrochim. Acta* **2009**, 54, 5942-
4
5 5948.
6
7

8
9 (29) Van Humbeek, J.-F. ; Proost, J. Current Understanding of Ti Anodisation: Functional,
10
11 Morphological, Chemical and Mechanical Aspects. *Corr. Rev.* **2009**, 27, 117-204.
12

13
14 (30) Likodimos, V.; Stergiopoulos, T.; Falaras, P.; Kunze, J.; Schmuki, P. Phase Composition,
15
16 Size, Orientation, and Antenna Effects of Self-Assembled Anodized Titania Nanotube
17
18 Arrays: A Polarized Micro-Raman Investigation. *J. Phys. Chem. C* **2008**, 112, 20574.
19
20

21
22 (31) Crawford, G. A.; Chawla, N. Tailoring TiO₂ Nanotube Growth During Anodic Oxidation
23
24 by Crystallographic Orientation of Ti. *Scr. Mater.* **2009**, 60, 874–877.
25
26
27
28
29
30
31
32
33
34
35
36
37
38
39
40
41
42
43
44
45
46
47
48
49
50
51
52
53
54
55
56
57
58
59
60

Table of Contents Graphic and Synopsis



Highly ordered TiO₂ nanotube arrays are produced by self-organized anodic growth. The influence of the underlying Ti substrate orientation on the nanotube growth rate is studied. Nanotubes with the highest aspect-ratio are found on substrate planes that have low atomic surface densities, nanotube formation is inhibited on Ti(001) oriented grains.

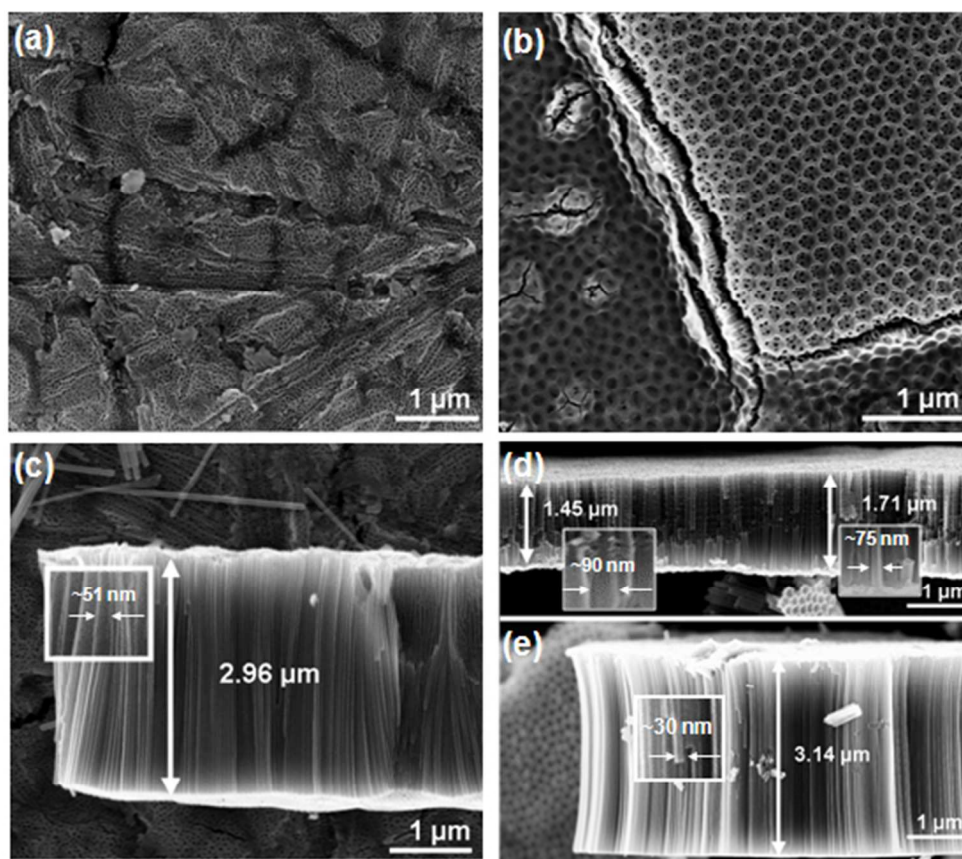


Figure 1: SEM top views and cross-sections of TiO₂ nanotubes grown in glycerol with 0.25wt.% NH₄F at 20 V for 6 hours on non-electropolished (a,c) and on electropolished (b,d,e) Ti substrates. In panel (d), the nanotube layer is flipped upside down, the nanotube bottoms showing ripples (see left inset in (d)).
48x42mm (300 x 300 DPI)

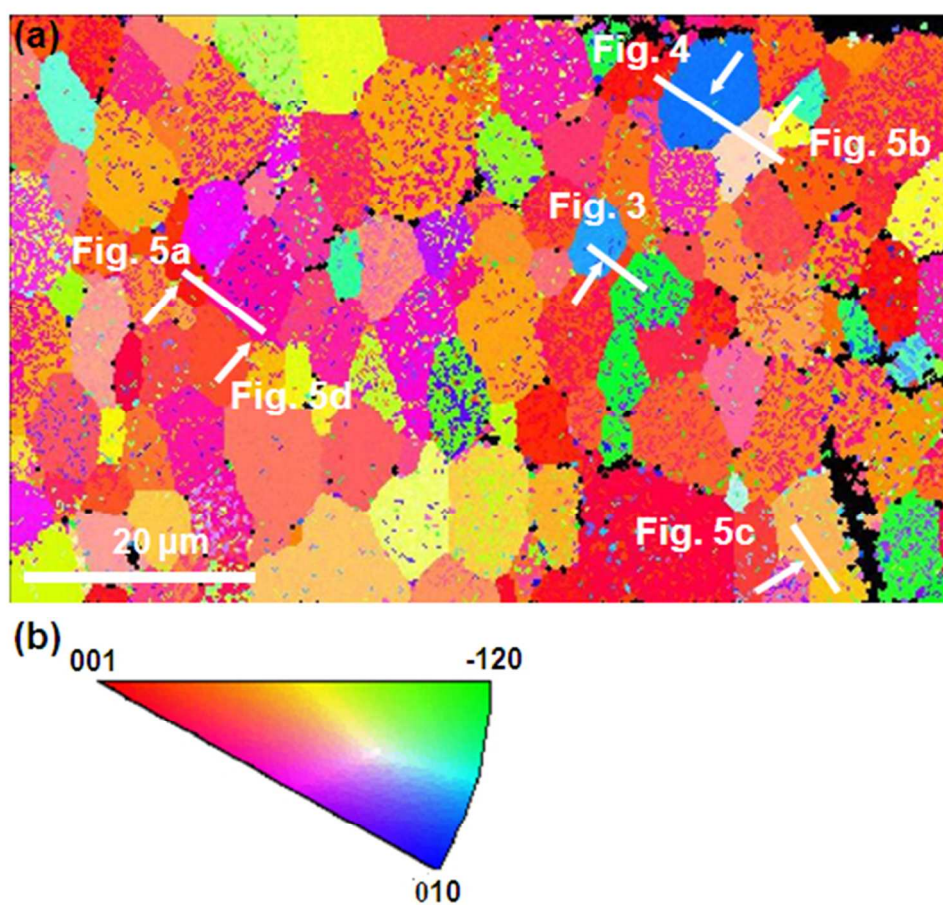


Figure 2: (a) Inverse pole figure (IPF) of the area where cross sections of the nanotubular film have been investigated with SEM: all cross sections are marked. (b) color legend for the IPF explaining the crystallographic orientations (orientations of the vertices refer to substrate planes).
46x43mm (300 x 300 DPI)

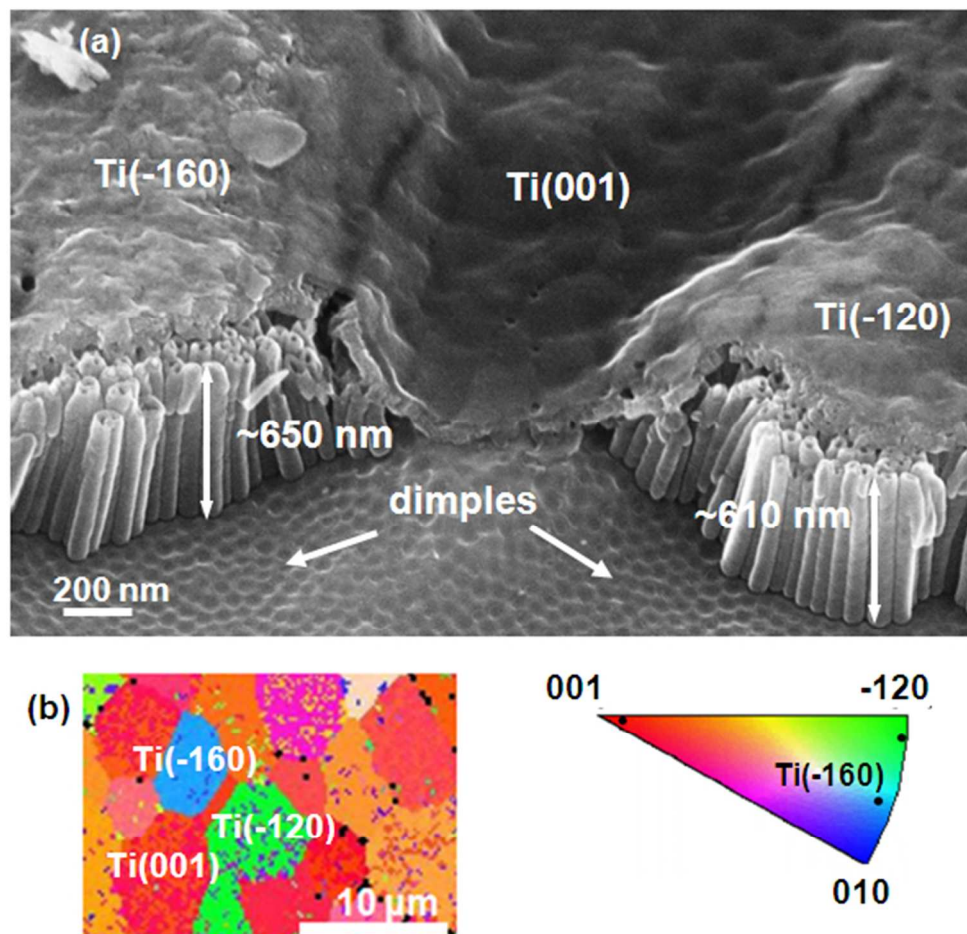


Figure 3: (a) Cross section of anodic TiO₂ nanotubes grown in glycerol with 0.25 wt.% NH₄F at 20 V for 6 hours on Ti(-160), Ti(001) and Ti(-120) oriented grains. (b) EBSD map and stereographic triangle showing the positions of substrate grains underlying the nanotubular oxides.
51x48mm (300 x 300 DPI)

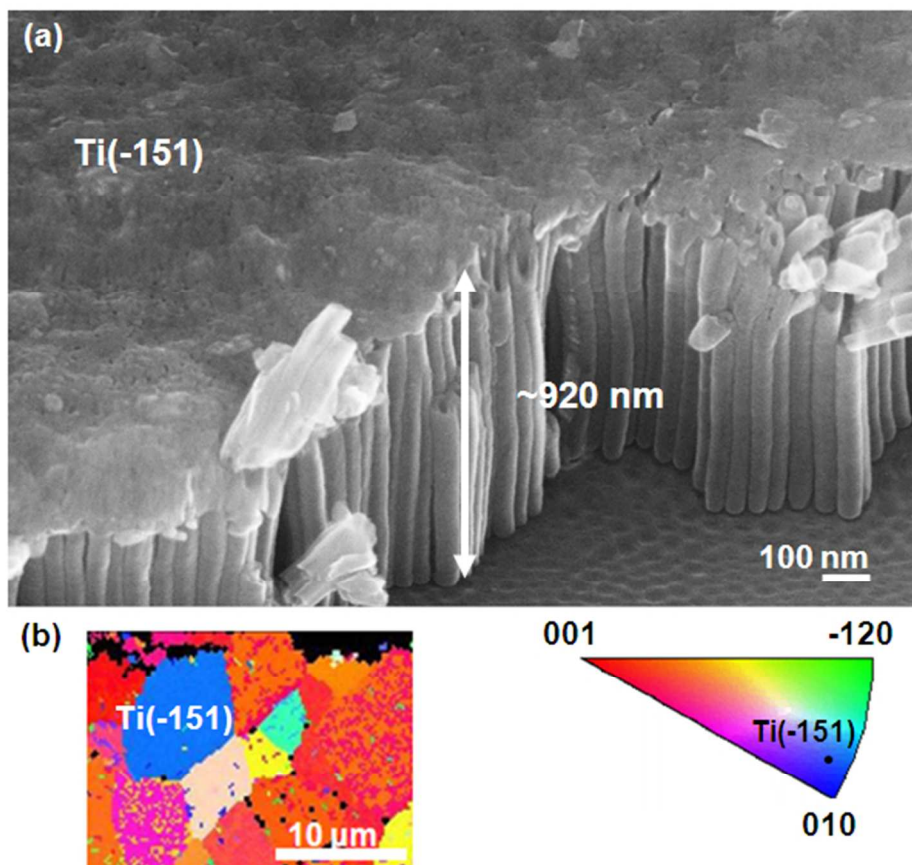


Figure 4: (a) SEM cross section of anodic TiO₂ nanotubes grown in glycerol with 0.25 wt.% NH₄F at 20 V for 6 hours on a Ti(-151) oriented grain. (b) EBSD map and stereographic triangle showing the position of the substrate grain underlying the nanotubular oxide.
55x47mm (300 x 300 DPI)

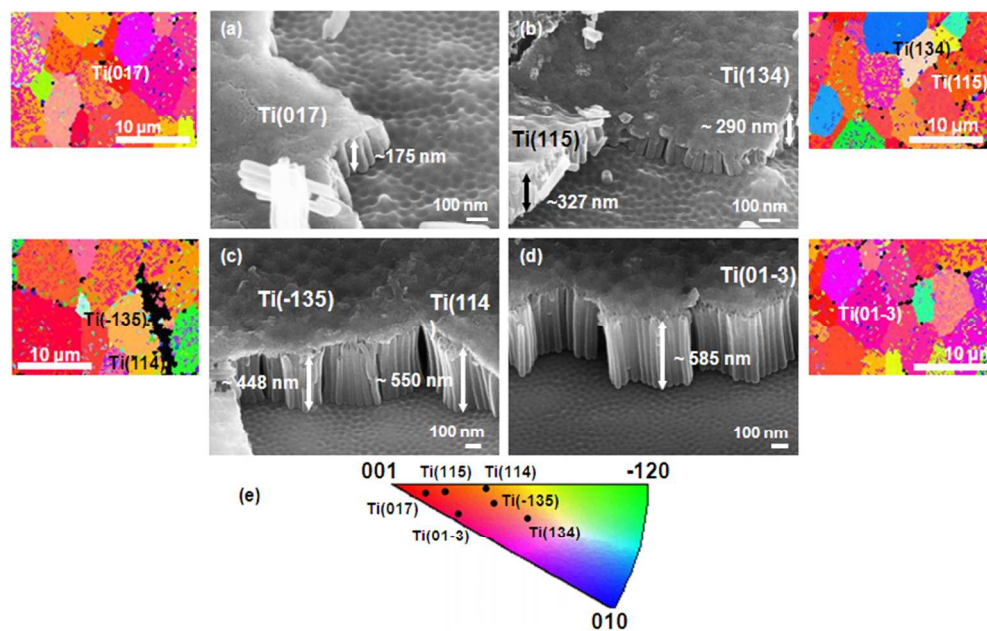


Figure 5: SEM cross sections of TiO₂ nanotubes grown in glycerol with 0.25 wt % NH₄F at 20V for 6 hours on differently oriented grains: (a) Ti(017), (b) Ti(115) and Ti(134), (c) Ti(-135) and Ti(114) and (d) Ti(01-3) (b) EBSD map and stereographic triangle showing the positions of substrate grains underlying the nanotubular oxides.

74x47mm (300 x 300 DPI)

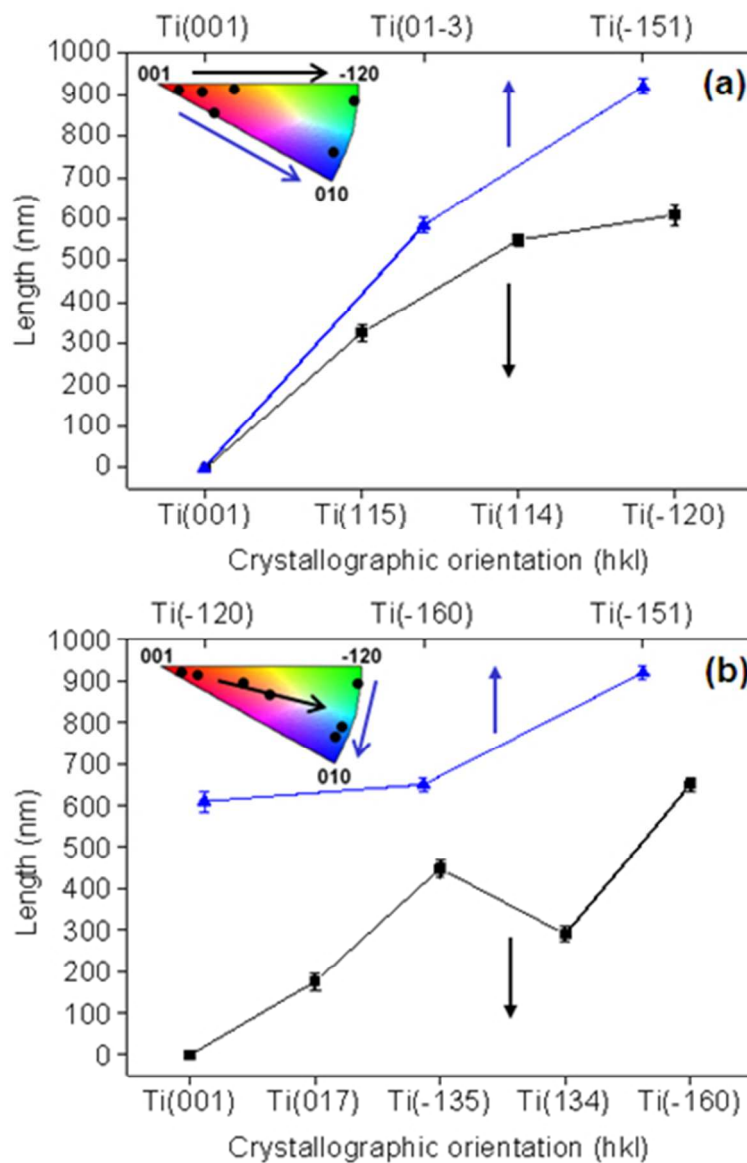


Figure 6: TiO₂ nanotube lengths for anodic films grown in glycerol with 0.25 wt% NH₄F for 6 hours at 20V on differently oriented substrate grains (standard deviations refer to length variations inside the same substrate grain). Change of plane orientations (a) along upper (black curve) and lower (blue curve) edges, (b) from (-120) to (010) (blue curve) and through the high-index inner planes (black curve) of the IPF color legend.

42x55mm (300 x 300 DPI)

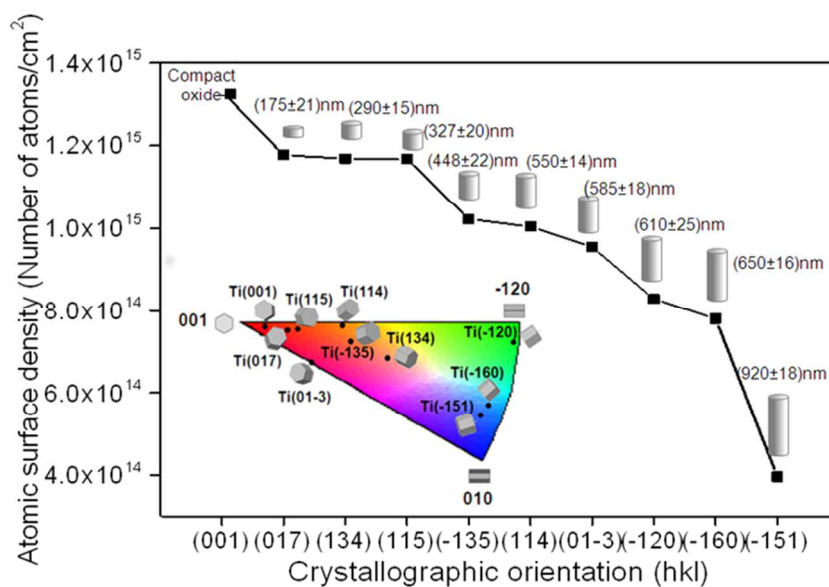
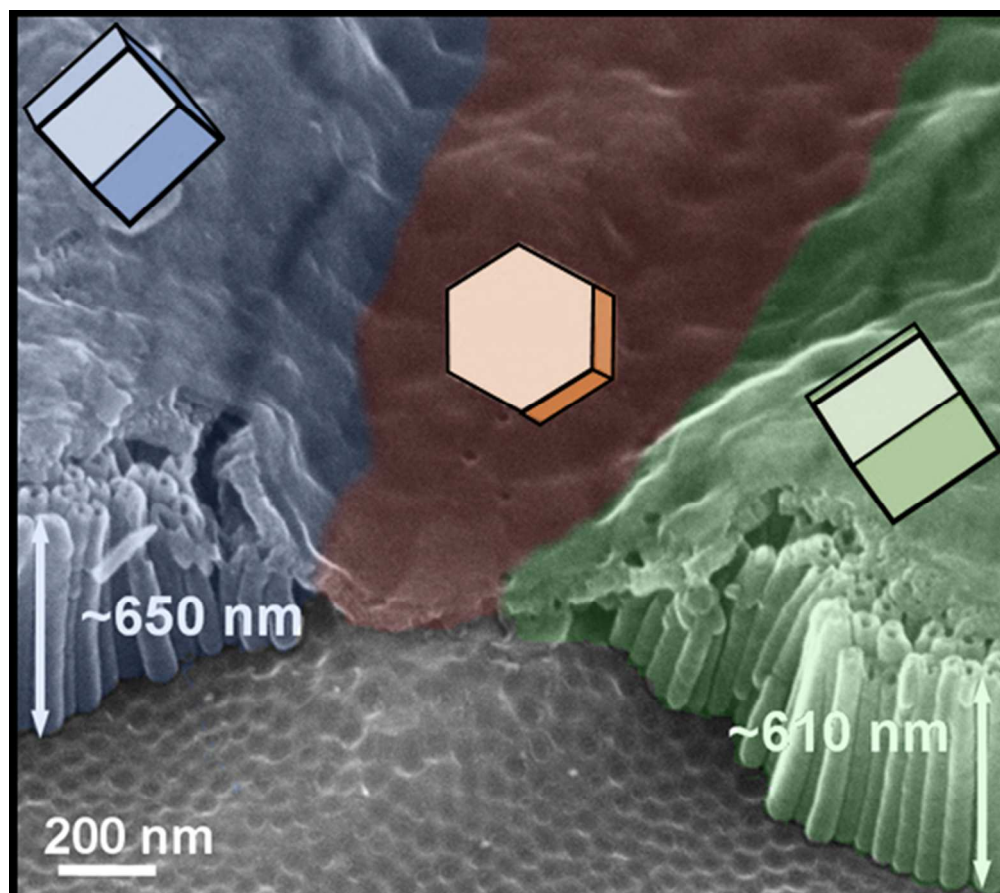


Figure 7: Atomic surface densities of Ti metal substrate planes and their correlation with TiO₂ nanotube lengths (standard deviations refer to length variations inside the same substrate grain), connecting lines are inserted as guide for the eye. Inset: orientation of hexagonal 3D unit cells of Ti substrate grains determined from Euler angles obtained with EBSD.

75x47mm (300 x 300 DPI)



ToC Graphic
45x40mm (300 x 300 DPI)